Talanta 82 (2010) 733–738

Contents lists available at ScienceDirect

Talanta

journal homepage: www.elsevier.com/locate/talanta

A cataluminescence gas sensor based on nanosized V_2O_5 for tert-butyl mercaptan

Huili Zhang, Lichun Zhang, Jing Hu, Pingyang Cai, Yi Lv*

Key Lab of Green Chemistry & Technology of MOE, College of Chemistry, Sichuan University, No. 29, Wangjiang Road, Chengdu, Sichuan 610064, China

ARTICLE INFO

Article history:
Received 1 March 2010
Received in revised form 13 May 2010
Accepted 15 May 2010
Available online 24 May 2010

Keywords:
Cataluminescence
Gas sensor
Vanadium pentoxide
Tert-butyl mercaptan

ABSTRACT

This work proposed a gas sensor for the determination of tert-butyl mercaptan, one of the highly toxic volatile sulfur compounds, which was based on cataluminescence emission during its catalytic oxidation on the surface of nanosized V_2O_5. The cataluminescence characteristics and the optimum conditions, including the morphology of sensing material, the wavelength of cataluminescence emission, the oxygen flow rate and working temperature were investigated in detail. Under the optimized conditions, the calibration curve of the relative cataluminescence intensity versus the concentration of tert-butyl mercaptan vapor was made, with the linear range of 5.6–196 $\mu g\,mL^{-1}$ and the detection limit of 0.5 $\mu g\,mL^{-1}$ ($S/N = 3$). The relative standard deviation (R.S.D.) ($n = 5$) of relative cataluminescence intensity for 84 $\mu g\,mL^{-1}$ tert-butyl mercaptan was 3.6%. There is no or weak response to some common substances, such as formic acid, alcohol (methanol, ethanol, propanol, isopropanol, *n*-butanol, isoamyl alcohol), *o*-dichlorobenzene, acetonitrile, ethyl acetate, aldehyde (formaldehyde, acetaldehyde and propanal), 1,2-dichloroethane and ammonia. Furthermore, the proposed sensor was successfully used for determining tert-butyl mercaptan in four artificial samples, with a good recovery. The results demonstrated that the proposed gas sensor had a promising capability for the tert-butyl mercaptan in routine monitoring.

1. Introduction

Recently, there has been a growing interest in monitoring of volatile sulfur compounds (VSCs) due to their potential of causing a range of health and environmental problems [1]. VSCs are usually produced by the metabolism of a microscopic organism, and generated in the processes of handling or degradation of organic material, such as slaughtering, sewage treatment, biogas production and landfilling [2], furthermore, these bad-smelling substances can also be oxidized to SO_2 and sulfate in the troposphere and induce a global atmospheric problem of acidic precipitation [3]. Nowadays, a growing body of scientific evidence has indicated that exposure to even trace levels will cause some damage to health [4], e.g. respiratory and neuropsychological diseases. Especially, tert-butyl mercaptan as one of the VSCs, which has highly toxic and offensive odor for eyes, upper respiratory tract and skin, can cause headache, naupathia, anaesthesia, even unconsciousness and death.

Up to the present, many techniques have been attempted for the determination of VSCs. Gas chromatography (GC) with a sulfur-selective detector is the general method, for example, gas chromatography with a flame photometric detector (GC-FPD) [5] or gas chromatography with the pulsed flame photometric detector (GC-PFPD) [6]. Gas chromatography with the sulfur chemiluminescence detector (SCD) has high selectivity and a wide linear range [7], in which the sulfur-containing substances can be converted into SO_2 in a hydrogen/oxygen furnace and subsequent ozone-induced chemiluminescence. Gas chromatography with atomic emission detection (GC-AED) [8] or mass spectrum (GC–MS) [9,10] has also been attempted for the determination of VSCs, despite of the high cost and highly skilled analysts. Therefore, there are still very strong demands for novel, simple, rapid and stable methodologies, especially a gas sensing system [11], for monitoring the trace tert-butyl mercaptan.

It is worth mentioning here that chemiluminescence generated on the surface of nanomaterials has been investigated as a promising transduction principle [12,13] for gas sensors due to its simplicity, sensitivity and fast response. In 1976, Breysse et al. [14] observed luminescence phenomenon on the surface of thoria during the catalytic oxidation of carbon monoxide, and established the concept "cataluminescence" for the first time. In 1990s, the cataluminescence (CTL) gas sensors for the determination of trace organic vapor (e.g. ethanol and acetone) using the bulks sensing material γ-Al_2O_3 or γ-Al_2O_3 doped with Dy^{3+} were developed by Nakagawa and co-workers [15,16]. At the same time, the application of nanomaterials to the design of cataluminescence gas sensors became one of the most active research fields because of their high activity, good selectivity, tremendous specific surface and small size [17]. Zhang and co-workers poured much endeavor on the CTL studies and established a series of gas sensors and sensor arrays by use

* Corresponding author. Tel.: +86 28 8541 2798; fax: +86 28 8541 2798.
E-mail address: lvy@scu.edu.cn (Y. Lv).

0039-9140/$ – see front matter © 2010 Elsevier B.V. All rights reserved.
doi:10.1016/j.talanta.2010.05.040

of different catalytic nanomaterials, for example, ethanol gas sensor based on nanosized TiO_2 [18] and $SrCO_3$ [19], NH_3 gas sensor based on $LaCoO_3$ [20], trimethylamine gas sensor based on Y_2O_3 [21], and cataluminescence-based gas sensor arrays [22–25] for volatile organic compounds. Lu and co-workers have also developed a sensitive gas sensor based on the functioned zeolite for the detection of *n*-hexane [26]. Cao et al. have also developed an ether gas sensor based on nanosized $ZnWO_4$ [27]. In our previous works, several CTL sensors were also developed, such as carbon disulfide sensor based on CeO_2 nanoparticles [28], acetone gas sensor based on micro-octahedra Mn_3O_4 [29], ethyl ether gas sensor based on borate glass [30], and ethanol gas sensor based on nanosized ZnO [31].

Here, a CTL gas sensor based on the nanosized vanadium pentoxide for the determination of tert-butyl mercaptan has been investigated. In order to obtain the suitable sensing material for tert-butyl mercaptan, dozens of materials including $BaCO_3$, MgO, ZnO, V_2O_5, La_2O_3, Fe_2O_3, etc. were explored as the candidate of sensing material, the preliminary experiments indicated that the cataluminescence emission could be obtained during the oxidation of tert-butyl mercaptan vapor on the surface of V_2O_5. Thus, much endeavor has been made to improve the capability of the V_2O_5 sensing material via synthesis in the present work. The nanosized vanadium pentoxide, which was widely applied to catalysis and electro-chemistry due to the versatile redox-dependent properties [32], was obtained by hydrothermal synthesis. The preliminary experiments showed that the strong CTL emission can be obtained when the vapor of tert-butyl mercaptan passes through the surface of nanosized vanadium pentoxide under catalytic reaction temperature. Based on this phenomenon, we proposed a novel gas sensor for determining the tert-butyl mercaptan.

2. Experimental

2.1. Reagents

All reagents were analytical reagent grade. Tert-butyl mercaptan was obtained from Shanghai Aladdin Co. Ltd. (Shanghai, China), and the others were purchased from Chengdu Kelong Co. Ltd. (Chengdu, China). Standard solution of tert-butyl mercaptan is sealed and stored in the refrigerator always. When used, several milliliters of standard solution was transferred to a small vial and sealed as the working solution in the fume hood. All experimental operations of the determination process were carried out in the hood for safty. Different concentration samples were prepared by the following: the sample was injected into a 30 mL airtight bottle, and the temperature of bottle (100 °C) was controlled by a homemade heating system, then the sample vapor was introduced into the cataluminescence chamber of the detection system.

2.2. Synthesis of V_2O_5 nanoparticles

The nanosized vanadium pentoxide was synthesized by a typical hydrothermal synthesis methodology. The detailed synthesis procedure was approximately described as follows: NH_4VO_3 (0.8775 g) was dissolved in 30 mL water in a 60 mL polytetrafluoroethylene (PTFE, Teflon) autoclave equipped with a stainless steel shell, then HNO_3 (9 mL 2 mol L^{-1}) was added drop-wise with continuous stirring. Subsequently, the autoclave was maintained at 140 °C for 24 h. The final precipitate was washed with pure alcohol and water to remove possible residue, and then dried in 50 °C. In order to obtain V_2O_5 nanoparticles with different morphology, three final precipitates were calcined at different temperature (400, 500 or 600 °C) in a muffle furnace for 6 h, respectively.

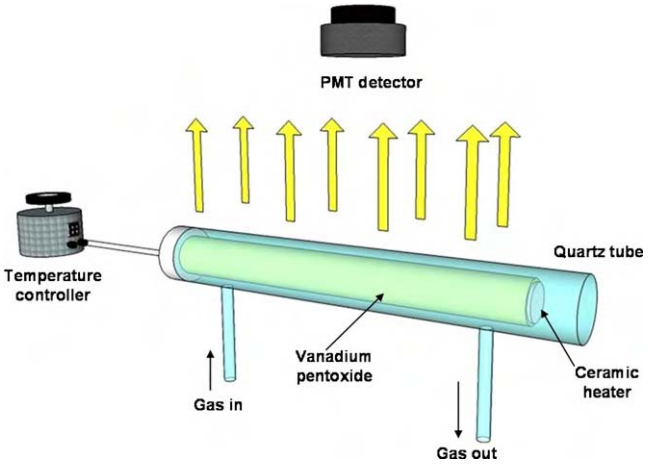

Fig. 1. Schematic diagram of the CTL sensing system.

2.3. Sensor apparatus

Fig. 1 shows the simplified schematic diagram of the main features for tert-butyl mercaptan sensing measurement in the present work. The CTL reaction system was made by sintering a 0.2-mm thick layer of V_2O_5 nanomaterials on a cylindrical ceramic tube (3.6 mm i.d.), which was inserted into a quartz tube (5.5 mm i.d). The ceramic tube was operated at the required temperature by a digital temperature controller. When the analyte (vapor of tert-butyl mercaptan) was driven through the surface of nano-V_2O_5 by air carrier, strong CTL emission can be observed. The CL signal at a certain wavelength was detected and recorded with a computerized BPCL ultra-weak chemiluminescence analyzer (Institute of Biophysics, Academia Sinica), equipped with a CR-105 photomultiplier tube (Hamamatsu), through variable interference optical filters that can be changed from 400 to 640 nm (400, 425, 440, 460, 490, 535, 555, 575, 620 and 640 nm). Data acquisition and treatment were performed with BPCL software running under Microsoft Windows XP.

2.4. Characterization

The powder X-ray diffraction (XRD) patterns were carried out on a Philips X'pert Pro MPD diffractometer (Philips Analytical,

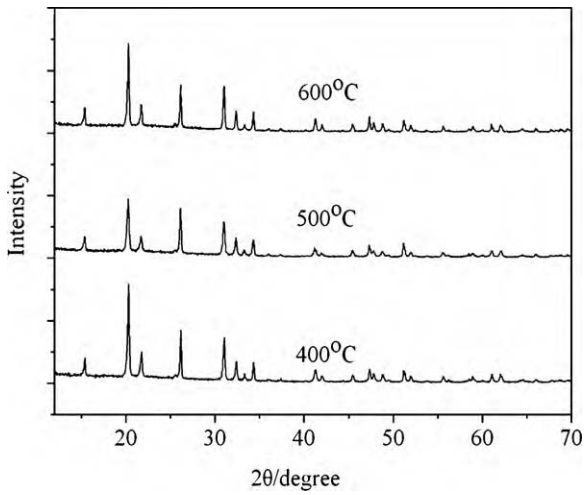

Fig. 2. XRD patterns of V_2O_5. The diffraction data were collected on a Philips X'pert Pro MPD diffractometer using Cu Kα radiation working at 40 kV and 40 mA. The samples were scanned from 12° to 70° (2θ) with a step size of 0.03°.

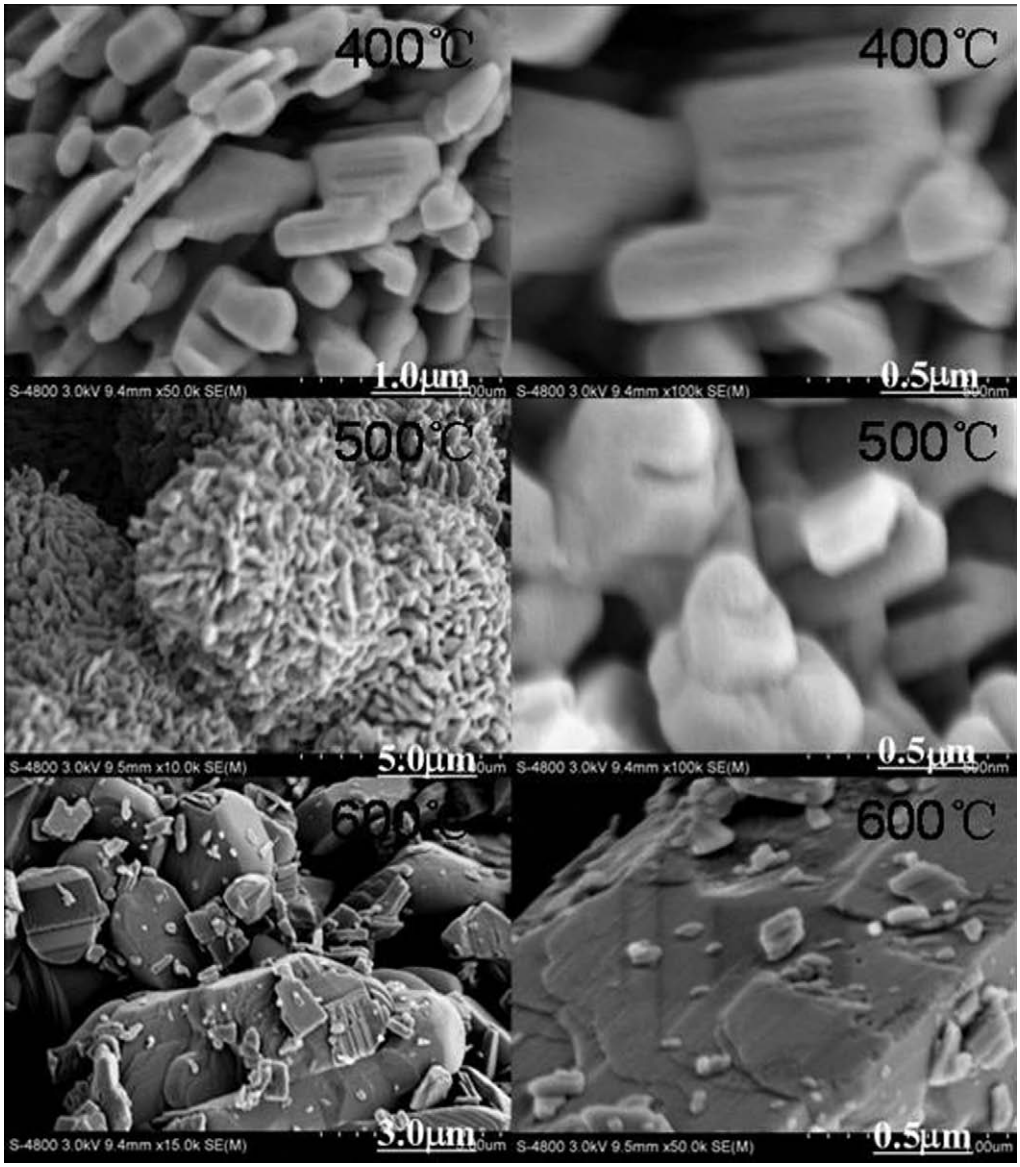

Fig. 3. SEM image of V_2O_5. The images were obtained throng a Hitachi (S-4800 I) scanning electron microscope (SEM) at an accelerating voltage of 3.0 kV. V_2O_5 was obtained from calcining precipitates in a muffle furnace for 6 h at (a) 400 °C, (b) 500 °C and (c) 600 °C.

Netherlands) equipped with a plumbaginous-monochromated Cu Kα radiation source working at 40 kV and 40 mA. The samples were scanned from 12° to 70° (2θ) with a step size of 0.03°. The morphology of synthesized V_2O_5 was examined on a Hitachi (S-4800 I) scanning electron microscope (SEM) at an accelerating voltage of 3.0 kV. In order to investigate the possible mechanism about the CTL reaction, a gas chromatography–mass spectrum (Shimadzu QP2010GC/MS system, Shimadzu Technologies, Japan) equipped with an Rtx-WAX column (30 m, 0.25 mm i.d., and 0.25 μm film thickness) was employed for detecting the resultant species in exhaust which was directly collected by a 2 L sample bag (Hede Biotechnology Company, Dalian, China).

3. Results and discussion

3.1. Structure and morphology

The XRD patterns of three synthesized V_2O_5 at different temperature (300, 400 and 600 °C) are shown in Fig. 2. The results indicated that three XRD patterns of V_2O_5 are mostly indexed to pure orthorhombic V_2O_5 (PDF #41-1426) with lattice parameters $a = 11.516$, $b = 3.5656$ and $c = 4.3727$. Profiles and strong peak positions are in good agreement with the XRD standard spectrum of V_2O_5 crystal. The morphologies of synthesized V_2O_5 are shown in Fig. 3. It can be seen that there are dramatic changes in size and surface morphologies of three synthesized V_2O_5, with an approximate tendency that the particle size increases along with the calcining temperature range of 400–600 °C. Furthermore, the later experiment indicates that the morphology of V_2O_5 has an obvious effect on the CTL response.

3.2. Effect of the V_2O_5 morphology

The CTL properties on the prepared nanosized V_2O_5 with different morphology were investigated by a continuous sampling of tert-butyl mercaptan vapor (28 μg mL^{-1}) with an air carrier flow rate at 400 mL min^{-1}. Under the working temperature 330 °C, the CTL emission through a series of interference (band-pass) optical filters in the range of 400–640 nm was recorded. The nanosized V_2O_5 with different morphology exhibits different CTL properties

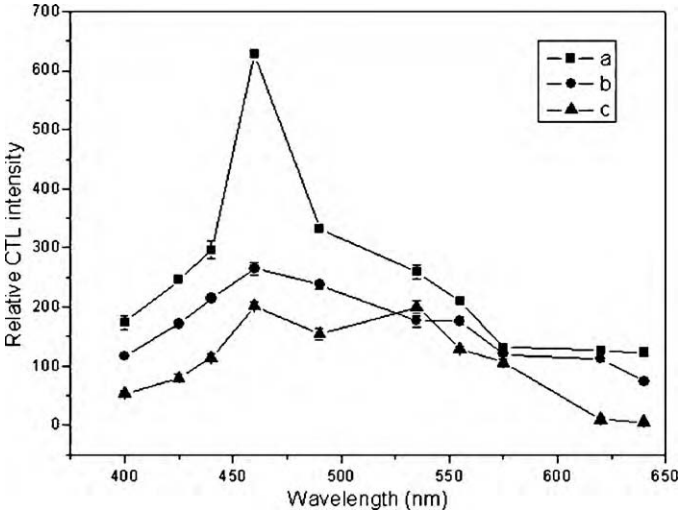

Fig. 4. CTL spectra emission on V_2O_5. Conditions: air carrier flow rate, 400 mL min^{-1}; working temperature, 330 °C. Error bar stand for ±S.D. (standard deviation). V_2O_5 was obtained from calcining precipitates in a muffle furnace for 6 h at (a) 400 °C, (b) 500 °C and (c) 600 °C.

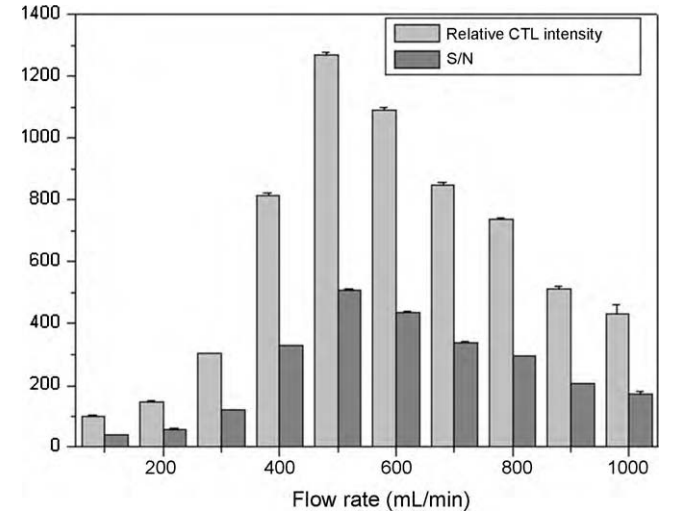

Fig. 5. The effect of air carrier flow rate on CTL. Conditions: working temperature, 330 °C; wavelength, 460 nm. Error bar stand for ±S.D. (standard deviation).

to tert-butyl mercaptan. As shown in Fig. 4, curves a, b and c are denoted as the CTL emission on the V_2O_5 calcined at 600, 500 and 400 °C, respectively. The results show that the V_2O_5 nanoparticle which was calcined at 600 °C (curve a) has the most strong CTL intensity with a maximum CTL wavelength 460 nm, also indicate that the nanosized V_2O_5 calcined at 600 °C is the excellent sensing material for the determination of tert-butyl mercaptan.

3.3. Effect of gas flow rate and working temperature

In this section, the working conditions including the carrier air flow rate and catalytic reaction temperature were investigated in detail. During the working temperature of 330 °C and the selected 460 nm band-pass filter, tert-butyl mercaptan vapor with the concentration of 28 μg mL^{-1} was introduced to study the effect of air carrier flow rate on the CTL intensity in the range of 100–1000 mL min^{-1}. From the results in Fig. 5, it can be seen that from 100 to 500 mL min^{-1}, CTL intensity and *S*/*N* (Signal-to-Noise Ratio, and noise is the width of baseline) increase with the increase of carrier flow rate. At the flow rate of 500 mL min^{-1}, the CTL intensity and *S*/*N* reach to the maximum, however, when flow rate is higher than 500 mL min^{-1}, the CTL intensity and *S*/*N* both decrease sharply. The reason probably relies on that the catalytic reaction between analyte vapor and sensing material would be insufficient at lower or higher air carrier flow rate. Therefore, the flow rate of 500 mL min^{-1} was chosen for the subsequent studies.

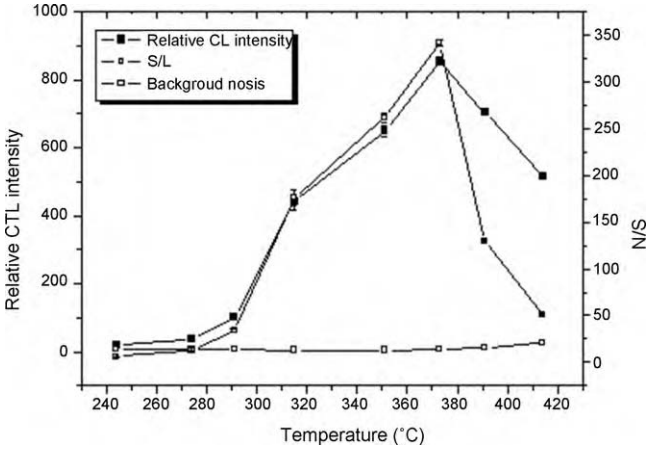

Fig. 6. The effect of working temperature on CTL. Conditions: air carrier flow rate, 500 mL min^{-1}; wavelength, 460 nm. Error bar stand for ±S.D. (standard deviation).

In the process of catalytic oxidation reaction, the working temperature usually plays an important role, thus the working temperature of the tert-butyl mercaptan on the nanosized V_2O_5 was optimized. The tert-butyl mercaptan vapor (28 μg mL^{-1}) was introduced at varied temperature. The CTL emission signal intensity and *S*/*N* versus the catalytic temperature at 500 mL min^{-1} air carrier flow rate under the wavelength of 460 nm is presented in Fig. 6. The results showed that the CTL intensity and *S*/*N* increases with the increase of working temperature from 244 to 351 °C. However, the CTL intensity and *S*/*N* reaches to the maximum at the working temperature of 351 °C. Therefore, 351 °C was chosen as the optimum working temperature in the following experiment.

3.4. Analytical characteristics and temporal CTL profiles of sensor

Under the selected optimum experiment conditions, the calibration curve of the relative CTL intensity was linear with the concentration of tert-butyl mercaptan in the range of 5.6–196 μg mL^{-1}, with a limit of detection (*S*/*N* = 3) of 0.5 μg mL^{-1}. The linear regression equation was $Y = -16.90 + 15.12X$ (correlation coefficient $R = 0.9998$; *X*, concentration of tert-butyl mercaptan (μg mL^{-1}); *Y*, the CTL intensity). Relative standard deviation (R.S.D., $n = 5$) was 3.6% for 84 μg mL^{-1} tert-butyl mercaptan.

CTL response profile was investigated by injecting different concentrations of tert-butyl mercaptan vapor under the optimized conditions. In Fig. 7, it can be seen that there are three corresponding CTL response profiles (a, b and c) which denote the CTL intensity for concentration of 28, 84 and 140 μg mL^{-1} of tert-butyl mercaptan, respectively. Three profiles are similar with each other, and the CTL intensity is proportional to the concentration of tert-butyl mercaptan. The signal rapidly increased from the baseline to the maximum value less than 5 s, on the other hand, the recovery time of the CL intensity for each curve is about 40 s. These results indicated that the proposed sensor has advantages of high throughput and excellent capability for routine monitoring.

3.5. Selectivity and stability

In order to evaluate the selectivity of the proposed gas sensor, a series of potential interference species with the same con-

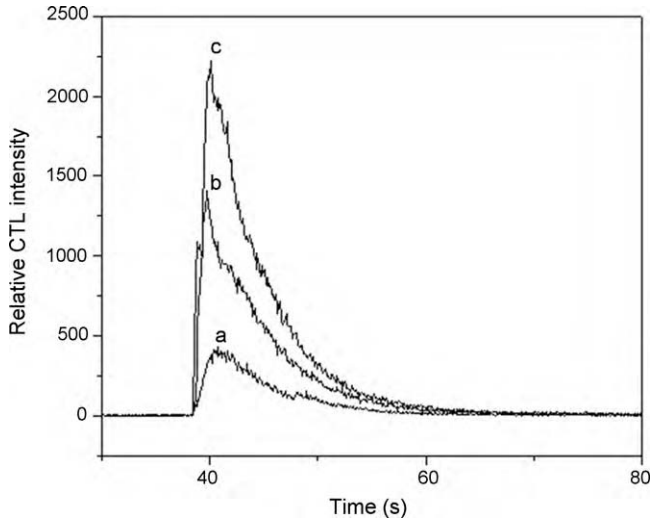

Fig. 7. Typical temporal profiles of CTL emission. Tert-butyl mercaptan vapor concentration: (a) 28 μg mL^{-1}; (b) 84 μg mL^{-1}; (c) 140 μg mL^{-1}. Conditions: wavelength, 460 nm; air carrier flow rate, 500 mL min^{-1}; working temperature, 351 °C.

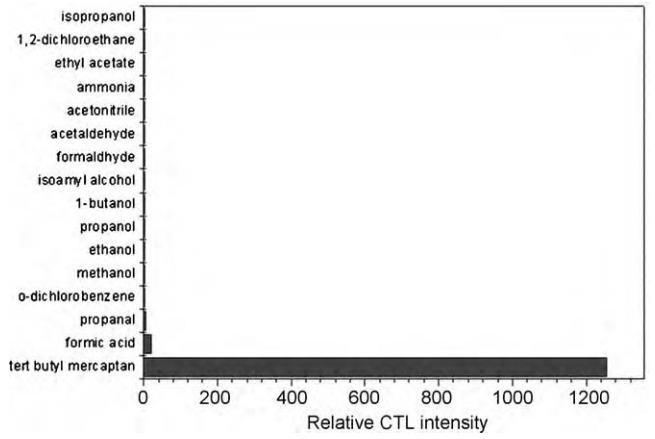

Fig. 8. Selectivity of tert-butyl mercaptan gas sensor. Conditions: wavelength, 460 nm; air carrier flow rate, 500 mL min^{-1}; working temperature, 351 °C.

centration of 84 μg mL^{-1} were investigated under the optimal experimental conditions. The species included formic acid, alcohol (methanol, ethanol, propanol, isopropanol, *n*-butanol, isoamyl alcohol), *o*-dichlorobenzene, acetonitrile, ethyl acetate, aldehyde (formaldehyde, acetaldehyde and propanal), 1,2-dichloroethane and ammonia. As shown in Fig. 8, all above-mentioned foreign species had no interference except formic acid had very weak CTL signal, and this result indicated that the present gas sensor exhibited a significantly high selectivity. The experiment about the stability and durability of this gas sensor was carried out by continuously sampling tert-butyl mercaptan vapor of 28 μg mL^{-1} into the sensor chamber under the optimal experiment conditions every day. After a week, no obvious change could be found, that is to say, the sensor had good stability and durability.

4. Sample analysis

The existence environment of tert-butyl mercaptan is usually complex, which probably lead to serious interference. In order to check the feasibility of this tert-butyl mercaptan gas sensor in real samples, four artificial samples were prepared and analyzed to estimate the validation of the proposed sensor. After complete vaporization, artificial samples were introduced into the sensing system under the optimal experimental conditions. As shown in Table 1, the results indicated the proposed gas sensor had a good capability for the measurement of tert-butyl mercaptan in routine monitoring.

Table 1
Analysis results of four artificial samples for tert-butyl mercaptan.

Sample no.	Mixture	Added values (μg mL^{-1})	Measured values (μg mL^{-1}, n = 3)
1	Tert-butyl mercaptan Formic acid	28 140	27.7 ± 0.5
2	Tert-butyl mercaptan *o*-Dichlorobenzene	14 112	13.5 ± 2.1
3	Tert-butyl mercaptan Formic acid *o*-Dichlorobenzene	14 28 28	14.1 ± 2.1
4	Tert-butyl mercaptan Formic acid Formaldehyde Ammonia	28 84 42 42	27.9 ± 2.3

5. Possible mechanism

According to the widely accepted chemiluminescence theory, it can be deduced that the excited intermediates are formed during the catalytic oxidation process of tert-butyl mercaptan by oxygen on the surface of V_2O_5, and light emission can be detected when these excited intermediates fall to the ground state. For the flame photometric detector, the possible chemiluminescence intermediate of sulfur-containing compounds was usually regarded as S_2^*, which has a maximum chemiluminescence peaks around 400 nm. Halstead and Thrush [33] observed an emission spectrum of the reaction of SO with ozone having both banded and continuum regions. Three electronically excited states of SO_2 [34] have been well characterized, the phosphorescent state provides a highly characteristic banded emission in the wavelength range of 380–470 nm. In the present work, with a series of (band-pass) optical filters as interference, the maximum CTL peaks are around 460 nm according to CTL profiles. Furthermore, GC–MS has been used to detect products from the catalytic oxidation of tert-butyl mercaptan on the surface of V_2O_5. The experiment showed that a large amount of SO_2 has been detected, which appear at 3.175 min. So, one of the products from the catalytic oxidation of tert-butyl mercaptan on the surface of V_2O_5 is SO_2. The possible mechanism is supposed as follow:

$$(CH_3)_3C - SH + O_2 \xrightarrow{V_2O_5} SO_2^* \rightarrow SO_2 + h\nu$$

6. Conclusion

Based on the luminescence emission from the catalytic oxidation of tert-butyl mercaptan on the surface of nano-V_2O_5, we developed a new gas sensor with the advantages of high selectivity, simplicity, fast response and satisfactory stability. The present gas sensor was successfully applied to determine trace tert-butyl mercaptan in four artificial samples, which demonstrated that it has the potential application for determination of tert-butyl mercaptan in industrial work place and other places.

Acknowledgement

The authors gratefully acknowledge the National Nature Science Foundation of China (No. 20875066) for financial support for this project.

References

[1] A. Szczurek, M. Maciejewska, B. Flisowska-Wiercik, L. Bodzoj, J. Environ. Monit. 11 (2009) 1942–1951.
[2] F. Lestremau, F.A.T. Andersson, V. Desauziers, J.L. Fanlo, Anal. Chem. 75 (2003) 2626–2632.
[3] T.J. Kelly, J.S. Gaffney, M.F. Phillips, R.L. Tanner, Anal. Chem. 55 (1983) 135–138.
[4] A. Moritz, D. Breuer, J. Environ. Monit. 10 (2008) 1454–1459.
[5] C.H. Yu, X. Li, B. Hu, J. Chromatogr. A 1202 (2008) 102–106.
[6] K.H. Kim, D.W. Ju, S.W. Joo, Talanta 67 (2005) 955–959.
[7] P.L. Burrow, J.W. Birks, Anal. Chem. 69 (1997) 1299–1306.
[8] C. Haberhauer-Troyer, E. Rosenberg, M. Grasserbauer, J. Chromatogr. A 848 (1999) 305–315.
[9] M.R. Ras, F. Borrull, R.M. Marce, Talanta 74 (2008) 562–569.
[10] M.R. Ras, R.M. Marce, F. Borrull, Talanta 77 (2008) 774–778.
[11] M. Seyama, Y. Iwasaki, S. Ogawa, I. Sugimoto, A. Tate, O. Niwa, Anal. Chem. 77 (2005) 4228–4234.
[12] R.A. Potyrailo, V.M. Mirsky, Chem. Rev. 108 (2008) 770–813.
[13] Y.Y. Su, H. Chen, Z.M. Wang, Y. Lv, Appl. Spectrosc. Rev. 42 (2007) 139–176.
[14] M. Breysse, B. Claudel, L. Faure, M. Guenin, R.J.J. Williams, T. Wolkenstein, J. Catal. 45 (1976) 137–144.
[15] M. Nakagawa, T. Okabayashi, T. Fujimoto, K. Utsunomiya, I. Yamamoto, T. Wada, Y. Yamashita, N. Yamashita, Sens. Actuators B: Chem. 51 (1998) 159–162.
[16] T. Okabayashi, T. Fujimoto, I. Yamamoto, K. Utsunomiya, T. Wada, Y. Yamashita, N. Yamashita, M. Nakagawa, Sens. Actuators B: Chem. 64 (2000) 54–58.
[17] J.J. Shi, Y.F. Zhu, X.R. Zhang, W.R.G. Baeyens, A.M. Garcia-Campana, Trac-Trends Anal. Chem. 23 (2004) 351–360.
[18] Y.F. Zhu, J.J. Shi, Z.Y. Zhang, C. Zhang, X.R. Zhang, Anal. Chem. 74 (2002) 120–124.
[19] J.J. Shi, J.J. Li, Y.F. Zhu, F. Wei, X.R. Zhang, Anal. Chim. Acta 466 (2002) 69–78.
[20] J.J. Shi, R.X. Yan, Y.F. Zhu, X.R. Zhang, Talanta 61 (2003) 157–164.
[21] Z.Y. Zhang, K. Xu, Z. Xing, X.R. Zhang, Talanta 65 (2005) 913–917.
[22] N. Na, S.C. Zhang, X. Wang, X.R. Zhang, Anal. Chem. 81 (2009) 2092–2097.
[23] N. Na, S.C. Zhang, S.A. Wang, X.R. Zhang, J. Am. Chem. Soc. 128 (2006) 14420–14421.
[24] X. Wang, N. Na, S.C. Zhang, Y.Y. Wu, X.R. Zhang, J. Am. Chem. Soc. 129 (2007) 6062–6063.
[25] Y.Y. Wu, N. Na, S.C. Zhang, X. Wang, D. Liu, X.R. Zhang, Anal. Chem. 81 (2009) 961–966.
[26] P. Yang, X.N. Ye, C.W. Lau, Z.X. Li, X. Liu, J.Z. Lu, Anal. Chem. 79 (2007) 1425–1432.
[27] X.A. Cao, W.F. Wu, N. Chen, Y. Peng, Y.H. Liu, Sens. Actuators B: Chem. 137 (2009) 83–87.
[28] Y.L. Xuan, J. Hu, K.L. Xu, X.D. Hou, Y. Lv, Sens. Actuators B: Chem. 136 (2009) 218–223.
[29] L.C. Zhang, Q. Zhou, Z.H. Liu, X.D. Hou, Y.B. Li, Y. Lv, Chem. Mater. 21 (2009) 5066–5071.
[30] J. Hu, K.L. Xu, Y.Z. Jia, Y. Lv, Y.B. Li, X.D. Hou, Anal. Chem. 80 (2008) 7964–7969.
[31] H.R. Tang, Y.M. Li, C.B. Zheng, J. Ye, X.D. Hou, Y. Lv, Talanta 72 (2007) 1593–1597.
[32] Y. Wang, G.Z. Cao, Chem. Mater. 18 (2006) 2787–2804.
[33] C.J. Halstead, B.A. Thrush, Photochem. Photobiol. 4 (1965) 1007–1013.
[34] R.J. Glinski, D.A. Dixon, J. Phys. Chem. 90 (1986) 3346–3353.